buildings

Article

Analysis of the Mechanical Properties of Cured Sludge by Alkaline Excitation of Phosphogypsum

Fu Wen [1], Ying Fan [1,*], Jingrong Wu [1] and Wenjie Yao [1,2]

1 School of Civil Engineering Architecture and the Environment, Hubei University of Technology, Wuhan 430068, China; 102110854@hbut.edu.cn (J.W.)
2 Wuhan Institute of Rock and Soil Mechanics, Chinese Academy of Sciences, Wuhan 430064, China
* Correspondence: 102111017@hbut.edu.cn

Abstract: Engineering slag is a green building material that meets the requirements of contemporary sustainable development, and the solidification technology of residue is particularly important in the practical engineering of resource utilization and environmental protection. In order to reuse the waste soil and industrial waste and reduce the construction cost, the stabilization effect of adding different contents of calcium oxide, blast furnace slag and phosphogypsum to the waste soil of a township road reconstruction project was studied. The unconfined compressive strength test of calcium oxide further clarified the solidification mechanism of residual soil and helped us to obtain the optimal curing ratio. The dry and wet cycle test simulated the influence of temperature and humidity changes on the appearance, quality, strength and water resistance in actual engineering. The experimental results show that the unconfined compressive strength of the sample reaches 1.273 MPa after 7 days of curing when the mixture of 4% calcium oxide (ratio to 100% plain soil) and 16% blast furnace slag (ratio to 100% plain soil) is mixed. When the three materials were mixed, the unconfined compressive strength of 4% calcium oxide (the ratio of 35% phosphogypsum and 65% plain soil) and 16% blast furnace slag (the ratio of 35% phosphogypsum and 65% plain soil) reached 1.670 MPa and 3.107 MPa at 7 and 28 days, respectively. The curing age has a significant promoting effect on the stability of loess. The dry and wet cycle test results conclude that the specimens have good durability and stability. The results of microstructure analysis shows that a large number of ettringite and C-S-H gel were formed in the gelling system, which not only makes the original soil more stable, but also acts as a part of filling pores, and the two work together to support the soil and improve the strength.

Keywords: engineering slag; industrial waste; unconfined compressive strength; dry–wet cycle; microstructure

check for updates

Citation: Wen, F.; Fan, Y.; Wu, J.; Yao, W. Analysis of the Mechanical Properties of Cured Sludge by Alkaline Excitation of Phosphogypsum. *Buildings* **2024**, *14*, 646. https://doi.org/10.3390/buildings14030646

Academic Editor: Dan Bompa

Received: 7 November 2023
Revised: 4 December 2023
Accepted: 8 December 2023
Published: 29 February 2024

1. Introduction

Currently, China is actively engaged in urban construction efforts, resulting in an increasing generation of construction residue during the process. The accumulation of such residues can potentially lead to the infiltration of harmful substances into soil and groundwater, thereby causing environmental pollution. Additionally, excessive residue accumulation may also encroach upon valuable land resources and restrict the city's development space. Measures that can be implemented include the rational planning of waste storage and recycling.

Through the work conducted by Xing et al. [1], including engineering geological mapping, drilling, in situ testing, and laboratory tests, the physical and mechanical properties as well as engineering geological characteristics of soft soil were determined. Additionally, the spatial distribution and physical properties of soft soil were analyzed. Zhang [2] investigated the causes of instability in engineering soft soil foundations. The research findings revealed that soft soil embankment foundations exhibit a high moisture content, a large pore ratio, medium–high compressibility, and medium–high sensitivity, among other characteristics. Consequently, it can be inferred that engineering soft soil also possesses attributes such as a high clay content, high compressibility, and low bearing capacity. Therefore, direct utilization of such construction residue as filling material is deemed unsuitable.

In order to solve the problem of the cost-effective utilization of engineering soft soil, scholars at home and abroad have carried out some studies, so that the solidification technology of engineering soft soil has made remarkable progress.

Huang and Zhou [3] investigated the hardening mechanism of cement-stabilized residual soil. The strength of cementitious reinforcements primarily derives from the cement hydration products' cementation process. Liang et al. [4] examined the stabilization of soft soil in Nansha, Guangzhou using lime and cement, comparing experiments with varying curing agent contents. They concluded that the strength of stabilized soft soil gradually increased with higher curing agent content and determined that a combination of 15% + 10% lime yielded optimal stabilization effects. Saadeldin [5] assert that clay is a fine-grained soil exhibiting high plasticity, easy consolidation, and low shear strength.

However, at present, traditional silicate cement consumes a large amount of resources and energy during its production and application. If cement is used as a building material for a long time and put into large batch production, it will not only produce a high project cost, but also cause a serious impact on the environment and will be harmful to the human body in the process of production and processing. Globally, cement production generates about 800 million tons of carbon dioxide equivalent by 2020, the equivalent of carbon dioxide emissions from all international air transport. In order to solve this series of problems, scholars at home and abroad have been actively exploring ways to reduce or replace cement.

Miao et al. [6] utilized the synergistic effect of semi-aqueous phosphogypsum (HPG), grey calcium powder and cement-cured raw phosphogypsum (RPG) to formulate a composite cementing material based on phosphogypsum (PBCM). Single-factor experiments were conducted to investigate the impact of the HPG content on the performance of PBCM slurry. Furthermore, an orthogonal experiment was carried out to examine the influence of each admixture on the strength and water resistance of PBCM. Dong et al. [7] utilized a modified β-phosphogypsum hemihydrate (MPG) consisting of 50% β-hemihydrous phosphogypsum, 23% slag, 15% phosphorus slag, 10% clinker, and 2% quick lime to effectively solidify and stabilize lead-bearing sludge. Their findings indicate that the MPG solidifying material exhibits significant curative properties on lead-bearing sludge, resulting in not only reduced cement consumption but also offering a novel avenue for the resource utilization of phosphogypsum. Bian et al. [8], based on the curing performance and mechanism of industrial waste slag, studied the curing soft soil of single blast furnace slag, phosphogypsum and cement; it was concluded that Portland cement exhibited a higher solidification effect compared to blast furnace slag and phosphogypsum. Furthermore, an optimal mass ratio of Portland cement, blast furnace slag, and phosphogypsum was determined by developing a compound coagulant formula with excellent solidification performance.

The aforementioned article has significantly contributed to the research on cement reduction, optimal ratio analysis, enhanced durability investigation, plasticity index control, etc., and elucidates the role of various additives in diverse scenarios. Furthermore, by reducing cement consumption, it is possible to fully exploit solid waste resources and transform them into valuable assets. Nevertheless, the substantial amount of cement still poses a significant environmental impact and there remains ample room for improvement in terms of curing effectiveness.

The present study employs three types of curing agents, namely calcium oxide, hemihydrate phosphogypsum, and blast furnace slag, as materials for solidification. By fully utilizing the waste products of phosphogypsum and blast furnace slag, this research aims to propose a cost-effective and environmentally friendly alternative to cement for stabilizing soft soil in engineering projects. Through two compounding tests, the optimal ratio of curing agent is determined after considering factors such as low cost and comparable curing effectiveness to cement. A superior compound coagulant formula is developed based on these findings, with its solidification performance extensively investigated [9–14]. Furthermore, selected samples with the best proportions are subjected to dry–wet cycle experiments following previous tests. Finally, scanning electron microscopy (SEM) analysis is employed to examine the microstructure of solidified soft soil and elucidate the mechanism behind this composite coagulant's efficacy. This approach effectively contributes towards environmental protection by utilizing waste materials while expanding options for road construction materials.

2. Experimental Materials, Experimental Apparatus and Experimental Protocols

2.1. Experimental Material

Soil: the specimen was selected from the section Z2K0 + 100−K0 + 245 in the road reconstruction project of 254 Provincial Road from Xinjiangkou Town of Songzi City to 355 Provincial Road in the town of Shimizu, with a depth of about 5 m. After collection, the soil mass was stored in a dry place, dried in batches, and then placed in a storage box. Figure 1 illustrates the topography of this specific area.

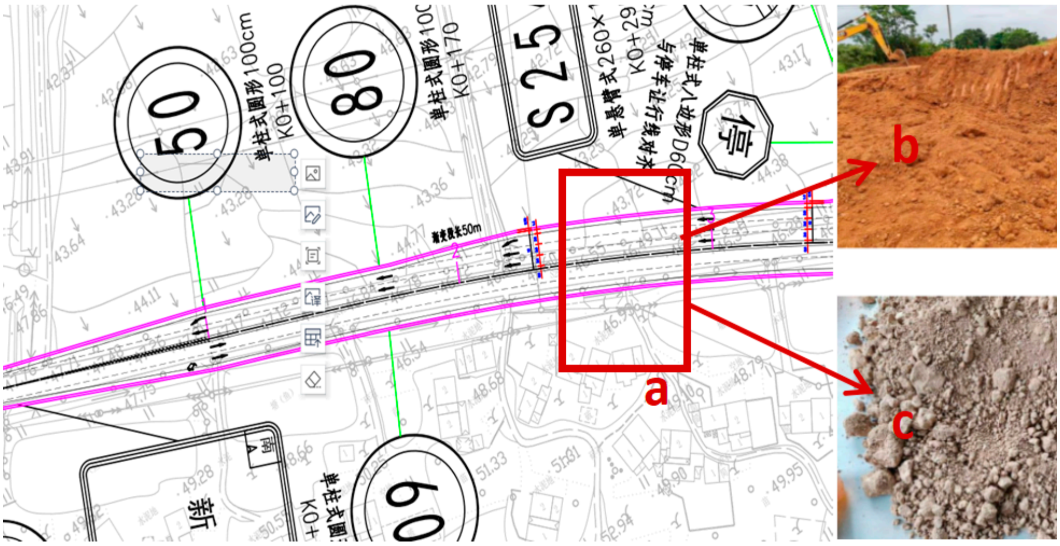

Figure 1. Soil samples (**a**) loess sampling section (**b**) soil samples before drying (**c**) soil samples after drying.

Sets of sieves: the set of sieves with sizes of 5 mm, 2 mm, 1 mm, 0.63 mm, 0.5 mm, 0.25 mm, 0.1 mm, 0.075 mm were measured and their set curves are shown in Figure 2, which shows that the curves are relatively flat, with a large difference in particle size, non-uniform particles, and a good gradation.

According to Highway Geotechnical Test Regulatio [15], laboratory testing was conducted on soil samples to determine their mechanical properties and chemical composition (refer to Tables 1 and 2). The results indicate that the excavated samples exhibit a favorable moisture content, non-uniformity coefficient > 5, curvature coefficient ranging from 1 to 3, and well-graded particle distribution. Additionally, the soil contains high levels of SiO_2, AI_2O_3, and CaO, which readily react with calcium oxide, blast furnace slag, and phosphogypsum—three common curing agents—resulting in a significant production of calcium silicate and ettringite. This reaction greatly enhances the effectiveness of the curing process.

Curing reagents: the selection of a commonly used curing agent calcium oxide, phosphogypsum, and blast furnace slag. Calcium oxide was from a chemical company in Tianjin, and had the appearance of a white slightly grey powder, with a density 3.30, and a certain degree of corrosiveness. Phosphogypsum and blast furnace slag are produced by a chemical plant in Wuhan and an iron and steel plant in Wuhan; the appearance of phosphogypsum and blast furnace slag are grey. The SO_3 and CaO content of phosphogypsum is 79.11%, while the SiO_2 and CaO of blast furnace slag account for 77.5%, and the chemical compositions of each reagent are shown in Table 3, respectively.

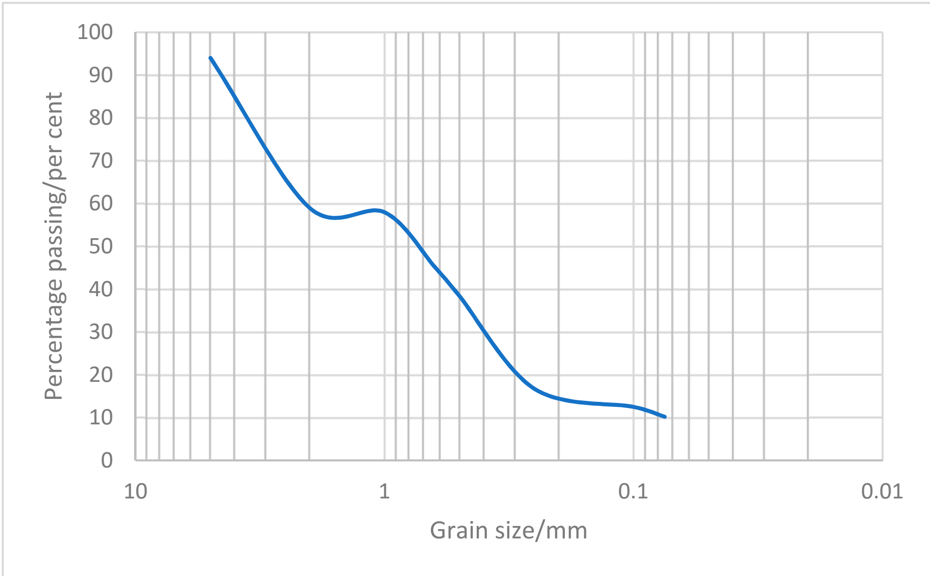

Figure 2. Particle size of soil samples.

Table 1. Mechanical parameters of soil samples.

Mechanical Parameter	Water Content in %	Liquid Limit % (WL)	Plastic Limit % (WP)	Plasticity Index	Maximum Dry Density (g/cm³)	Optimum Water Content%	Coefficient of Unevenness (CU)	Coefficient of Curvature (CC)
	17.3	35.8	17.4	18.4	1.76	16.7	6.7	1.67

Table 2. Chemical composition of soil.

Chemical Composition	SiO_2	Al_2O_3	CaO	Fe_2O_3	MgO	K_2O	The Rest
Percentage content (%)	55.2	12.1	9.5	4.4	2.3	1.3	15.2

Table 3. Chemical composition of calcium oxide, phosphogypsum and blast furnace.

CompositionChemical / Percentage Content (%)	SiO_2	AI_2O_3	CaO	Fe_2O_3	MgO	SO_3	MnO	The Rest
calcium oxide	1.2	0.6	85	/	5	/	/	8.2
phosphogypsum	8.26	0.99	33.36	0.86	/	45.75	/	10.78
blast furnace	37	8.7	40.5	2.3	6.5	0.01	0.65	4.34

2.2. Experimental Instruments

Dryer: The dryer is a type of equipment used for drying samples in the laboratory. The dryer has a voltage of 220 V and a power of 6000 W, with a temperature range of room temperature to 300 °C. It has a size of 500 mm × 600 mm. Its dimensions are 500 mm × 600 mm × 750 mm.

Compaction apparatus: The compaction apparatus is a type of equipment used for tamping experimental specimens, reducing the pore space of specimens and increasing the compactness of soil samples. In the unconfined compressive strength test, in order to obtain accurate and reliable test results, it is necessary to use the compaction method for the tamping of the test block in this experiment is used in the ordinary compaction mold, the size of 50 mm × 100 mm.

Jack stripper: a Hantang vertical hydraulic jack, with an approved load capacity of 10T, was used.

No side limit compressive strength test: for this test a WDW-10E microcomputer control electronic general testing machine from Wuhan Zhanhua Science and Technology Co.

2.3. Experimental Program

2.3.1. Specimen Preparation and Maintenance

According to the experimental specification [15], the treated soil sample is mixed with a specific proportion of reagents. Then, an optimal water content (certain proportion of laboratory water) is added, and the mixture is stirred at a constant speed for 5 min using a mixer. This ensures that each component combines uniformly with water to form a high-quality mixture. Subsequently, the mixture is loaded into a lightweight compacted steel mold measuring 50 mm × 100 mm (petroleum jelly needs to be evenly applied inside the mold initially). To prevent faults between each layer, it is necessary to shave each layer before loading it onto the next layer of mix. By repeating this process three times, a dense test block is formed which can then be pushed out using a jack. Finally, each test block is sealed with plastic wrap and tape and labeled accordingly. Additionally, two parallel samples are required for each test block. After preparation, all test blocks are placed under standard laboratory conditions (temperature: 20 ± 2 °C; humidity: 95%) for curing purposes, as depicted in Figure 3.

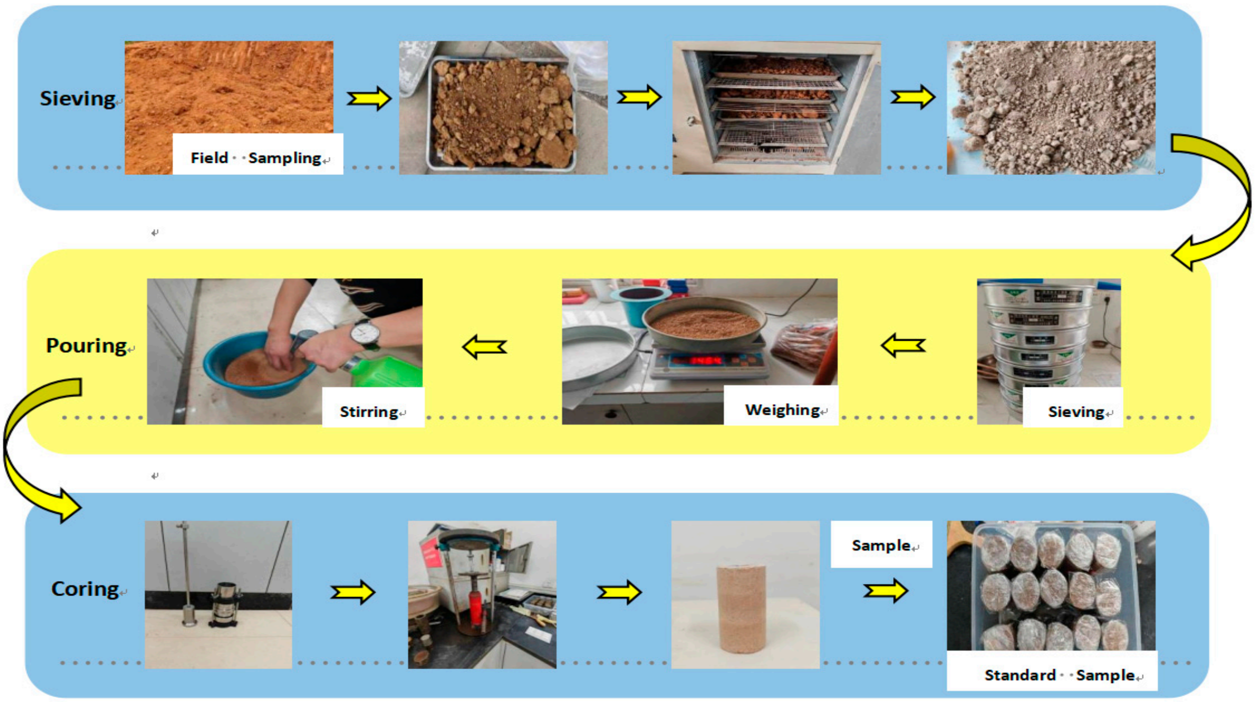

Figure 3. Flow chart of specimen preparation.

2.3.2. Unconfined Compressive Strength of UCS

In order to ensure optimal strength, two different curing agents, calcium oxide and blast furnace slag, were selected for single and compound mixing with a specific proportion of soil (maintained for 7 days). The resulting data changes were analyzed to determine the optimal ratio. Additionally, a certain proportion of hemihydrous phosphogypsum was mixed with soil samples and maintained for 7 and 28 days. After maintenance, test blocks were extracted according to the "Highway Geotechnical Test Regulations". Unconfined compressive strength tests were conducted using an electronic universal testing machine at a vertical loading rate of 1 mm/min. The test was stopped when obvious cracks appeared in the test block and the stress–strain curve reached its peak or tended towards stability. The peak data were recorded in Table 4 and must comply with the design specifications for highway cement concrete pavement [16].

Table 4. Experimental program for the unconfined compressive test.

	Curing Agent Mixing %			
Plain soil	0			
Mono-doped A1	1% CaO	2% CaO	4% CaO	6% CaO
Single-doped B1	8% GGBS	10% GGBS	12% GGBS	14% GGBS
Compound A2	8% GGBS + 1% CaO	8% GGBS + 2% CaO	8% GGBS + 4% CaO	8% GGBS + 6% CaO
Compound B2	10% GGBS + 1% CaO	8% GGBS + 2% CaO	8% GGBS + 4% CaO	8% GGBS + 6% CaO
Compound C2	12% GGBS + 1% CaO	8% GGBS + 2% CaO	8% GGBS + 4% CaO	8% GGBS + 6% CaO
Compound D2	14% GGBS + 1% CaO	8% GGBS + 2% CaO	8% GGBS + 4% CaO	8% GGBS + 6% CaO
E2 is the optimal ratio of the four schemes				
Compound A3	E2 + (90% soil + 10% PG)	Ratio of compounded A3-F3 CaO to GGBS is the ratio of soil + PG Maintenance 7 days, 28 days		
Compound B3	E2 + (85% soil + 15% PG)			
Compound C3	E2 + (80% soil + 20% PG)			
Compound D3	E2 + (75% soil + 25% PG)			
Compound E3	E2 + (70% soil + 30% PG)			
Compound F3	E2 + (soil 65% + 35PG%)			

2.3.3. Dry and Wet Cycle Test

The dry and wet cycle test is a commonly employed method in the field of solidified soil to investigate the stability of solidified soil under alternating wetting and drying conditions. Its objective is to simulate the natural drying and wetting cycles experienced by solidified soil, as well as evaluate its durability and erosion resistance. Considering the local circumstances, samples mixed with E2, C3, and F3 in three different ratios were extracted based on the aforementioned experiments. The samples were prepared following the mentioned methods and ratios. After curing for 28 days, they underwent 1, 3, and 5 dry–wet cycles (one set of test blocks was immersed in clean water at approximately 20 °C with a distance of about 30 mm between its surface and the water surface). They were soaked for 12 h before being removed. Subsequently, the specimens were either air-dried indoors or dehumidified using a water filter. Finally, they were placed in an electric blast drying oven at a temperature of 40 ± 2 °C for another 12 h to complete one dry–wet cycle. Unconfined compressive strength experiments were conducted to compare E2, C3, and F3 samples in terms of appearance changes, quality variations, and strength alterations while analyzing their underlying reasons.

2.3.4. Microscopic Experiments

After conducting the compressive strength test, a soil sample with an observation area of approximately 5 mm × 5 mm, a thickness less than 2 mm, and a flat surface was carefully selected. Subsequently, the sample underwent drying in an oven at 50 °C for a duration of 12 h. Following this treatment, the sample surface was subjected to pretreatment using vacuum metal spraying technology to minimize any interference caused by charge and discharge during scanning and recording of the sample. The European CarlZeiss Zeiss SIGMA field strain-emission scanning electron microscope was employed for this experiment, offering a resolution of 1.3 nm (20 kV) and 12.8 nm (1 kV), with an acceleration voltage ranging from 0.1 kV to 30 kV.

3. Experimental Results and Analysis

3.1. Calcium Oxide and Blast Furnace Slag Single Mixing Test

According to the results of the single mixing test depicted in Figure 4a,b, it can be observed that for both curing agents, namely calcium oxide and blast furnace slag, which were maintained for only 7 days, the compressive strength of specimens composed of calcium oxide and blast furnace slag increased with an increase in their mixing amount. However, after reaching a certain mixing amount, the compressive strength began to decrease. The highest recorded compressive strength was 0.610 MPa when the content of calcium oxide was 6%, while it reached its peak at 0.780 MPa when the content of blast furnace slag was 10%. In comparison to plain soil's compressive strength of 0.257 MPa, the addition of these two curing agents individually resulted in an increase in plain soil's compressive strength by approximately 137% and 204%, respectively.

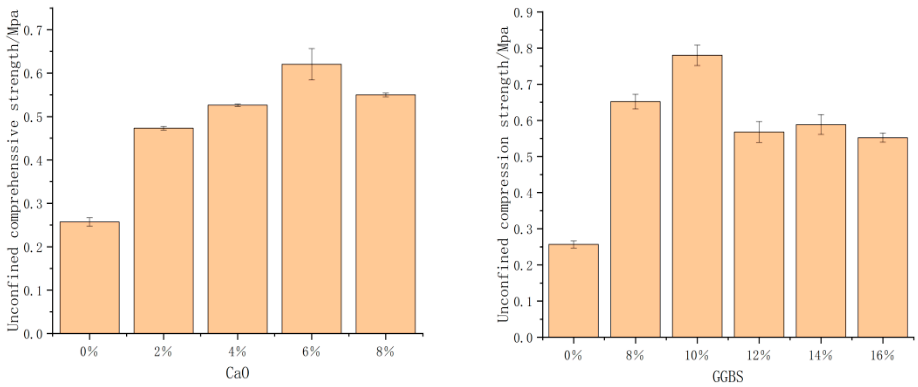

(**a**) (**b**)

Figure 4. Single blending test. (**a**) Calcium oxide single blending. (**b**) Blast furnace slag single blending.

The increase in strength is attributed to a series of physical and chemical reactions between calcium oxide and soft soil, encompassing ion exchange, crystallization, pozzolanic reaction, and carbonation. Initially, upon the addition of calcium oxide, hydration reaction takes place, resulting in the generation of abundant Ca^{2+} ions. These Ca^{2+} ions displace other ions within the soft soil through ion displacement to form hydrates such as calcium silicate hydrate (C-S-H) and calcium aluminate hydrate (C-A-H). The formation of these hydrates enhances the cementitious properties of soft soil, thereby improving its compressive strength. However, as the hydration reaction progresses, an excessive amount of $Ca(OH)_2$ crystals precipitate and fill the structure of soft soil, leading to internal pore formation. The presence of these pores diminishes the curing effect exerted by calcium oxide on soft soil. Consequently, the curing effect is influenced by precipitation of $Ca(OH)_2$ during the hydration reaction; while it increases compressive strength to a certain extent, excessive crystal precipitation results in pore formation, which reduces its overall effectiveness [17,18].

The single mixing experiment of blast furnace slag can produce a fibrous cementing material with specific structural characteristics and certain strength upon hydration, such as calcium silicate hydrate (C-S-H) and calcium aluminate hydrate (C-A-H) [19]. These cementing substances fill the pores in the solidified soil and form gelling, effectively achieving the purpose of consolidating soft soil. However, blast furnace slag (GGBS) has a stable network structure primarily composed of Si-O, Ca-O, and Mg-O bonds that are difficult to break down. Therefore, when adding only 10% blast furnace slag, the maximum compressive strength can only reach 0.780 MPa, which falls short of meeting engineering construction requirements.

3.2. Calcium Oxide and Blast Furnace Slag Compounding Test

According to the results of the calcium oxide and blast furnace slag compounding test, shown in Figure 5, the following can be observed when CaO is mixed. According to the test results depicted in Figure 5, it can be observed that when calcium oxide (CaO) and blast furnace slag (GGBS) are mixed, the following conditions arise. When the content of calcium oxide is 1%, there is no significant change.

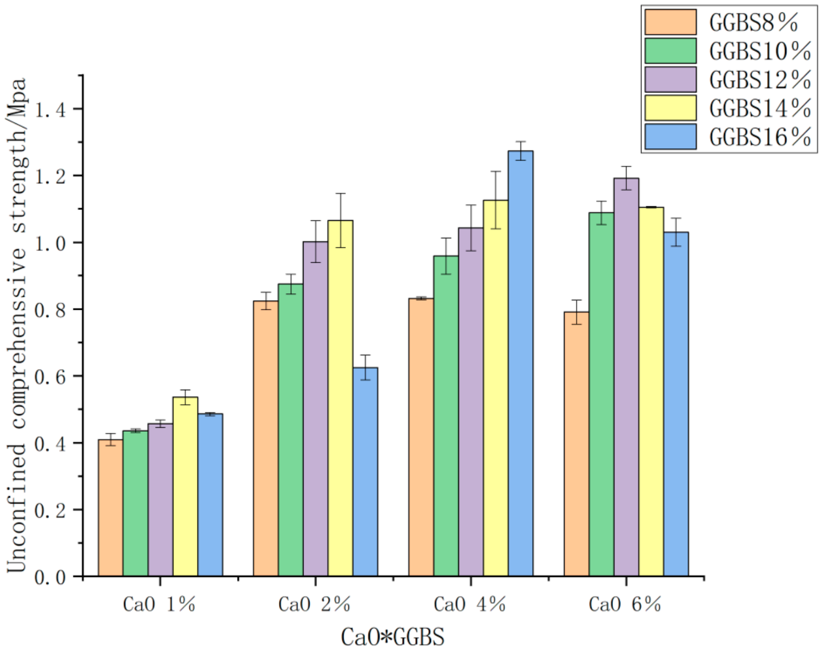

Figure 5. Strength change curve of calcium oxide and blast furnace slag compounded and maintained for 7d. (* = × means multiplication).

Increase in the strength of solidified soil: However, at calcium oxide contents of 2%, 4%, and 6%, there is a significant increase in strength for these three groups. The combinations of CaO at 2% with GGBS at 14%, CaO at 4% with GGBS at 16%, and CaO at 6% with GGBS at 12% exhibit the highest strength. The unconfined compressive strengths for these three composite ratios of solidified soil were, respectively, measured as follows: 1.065 MPa, 1.273 MPa, and 1.192 MPa. Compared to plain soil, these three combinations show improvements by factors of 314%, 395%, and 364%, respectively. With an increasing content of blast furnace slag (GGBS), the strength of solidified soil will be improved to a greater extent. However, as the content of calcium oxide gradually increases, the unconfined compressive strength initially increases but then decreases. In other words, increasing the calcium oxide content initially significantly improves the strength, but as it continues to increase, the unconfined compressive strength reaches an optimal point and subsequently declines. In tests involving mixing calcium oxide with blast furnace slag, a reasonable selection of their respective contents can significantly enhance the strength of the solidified soil; however, having excessively high levels of calcium may lead to a reduction in the curing effect.

When blast furnace slag (GGBS) is added to soft soil, the silicon–oxygen and calcium–oxygen bonds in GGBS are disrupted upon contact with water, resulting in the release of ions such as $(H_3SiO_4)^-$, $(H_4A1O_4)^-$, $(H_2SiO_4)^{2-}$, and Ca^{2+} into the water [20]. The water becomes enriched with Ca^{2+}, which facilitates the breakage of silica–oxygen bonds due to their relatively high bond energy. Additionally, aluminum and silicon substances on the surface of pelletized blast furnace slag powder contribute to this process. As hydroxide in the water is consumed, there is a gradual increase in pH value; however, this reaction occurs at a relatively slow rate and does not generate sufficient OH^- content for the extensive formation of hydrated calcium silicate. Conversely, when calcium oxide interacts with GGBS, it produces calcium hydroxide, which effectively enhances the OH^- content within the soil. This leads to the accelerated breaking of Si-O and Al-O bonds while promoting hydration reactions that result in an abundance of AI_2O_3 and SiO_2 hydration compounds. Consequently, these reactions expedite hydration processes and improve the overall strength [21].

3.3. Calcium Oxide, Blast Furnace Slag and Phosphogypsum Compound Mixing Test

The experimental results presented in Figure 6 demonstrate that the properties of the mixed soil are significantly influenced by the content of the curing agent and curing age, directly impacting the engineering properties of the cured mixed soil. After a 7-day curing period, it was observed that an increase in phosphogypsum content initially led to a slow rise in the compressive strength of the cured mixed soil, followed by a gradual decrease. At a phosphogypsum content of 20%, the solidified soil sample exhibited its lowest strength value at 1.148 MPa. However, as the phosphogypsum content continued to increase, the strength gradually improved but at a relatively slower rate until reaching stability. When using a phosphogypsum content of 35% with soil at a mixing ratio of 65% (PG*Soil), the solidified soil sample achieved its highest strength value at 1.670 MPa. Compared to plain soil, this optimal combination involving calcium oxide, blast furnace slag, hemihydrous phosphogypsum and plain soil resulted in an impressive increase in strength by 550% after seven days of curing. Furthermore, compared to samples without phosphogypsum, there was also an additional increase in strength by 31.2%. Based on these research findings, an optimum ratio for calcium oxide, blast furnace slag and hemihydrous phosphogypsum can be determined after seven days of maintenance for practical applications as an alternative material meeting medium and light traffic base requirements for certain pavements.

The results indicate that the unconfined compressive strength curve of the 28-day cured test block exhibits a more pronounced upward trend and a relatively moderate downward trend compared to that of the 7-day cured test block. At a phosphogypsum content of 10%, the solidified soil sample reaches its lowest strength.

It had a value of 2.175 MPa after 28 days of curing. Subsequent strength does not exhibit any significant upward trend with the gradual increase in phosphogypsum content, except when it reaches a content of 35%, where the solidified soil sample achieves its highest strength value of 3.107 MPa. Compared to their respective strengths during the initial 7-day curing period, there is an average increase in strength by percentages: 83%, 80%, 118%, 76%, 84% and 86%. On average, there is an overall increase in strength by approximately 87.8 percent. In summary, age has a certain influence on unconfined compressive strength. The test blocks cured for 28 days demonstrate a more evident upward trend as the phosphogypsum content gradually increases compared to those cured for only seven days, resulting in an overall higher level of strength. This indicates that extending the curing time can further enhance the compressive mixed soil.

When the phosphogypsum content is relatively low, phosphogypsum acts as a curing agent during the curing process, exhibiting a reaction mechanism similar to that of cement and phosphogypsum [22–24]. The hydration reaction of cement produces calcium hydroxide, calcium silicate, calcium chlorate, and other products. Upon formation of these hydration compounds, some continue to undergo hardening reactions to form a cement stone skeleton, while others react with surrounding clay particles through ion exchange, agglomeration, and hardening reactions. This significantly enhances the strength of the solidified soil. Simultaneously, the expanding material fills in the pores of the solidified soil, increasing its density and strength. However, the excessive generation of expansive mineral components (such as ettringite) may lead to the destruction of the calcium silicate formed by quicklime's hydration reaction and subsequently result in the decreased strength of solidified soil [25,26]. When there is a high content of phosphogypsum present, it no longer functions solely as an additive but also becomes part of the solidified soil structure. Compared to soil particles themselves, phosphogypsum has a smaller particle size, which gradually increases sanding within the soil matrix, leading to increased pore volume and stabilization in structure.

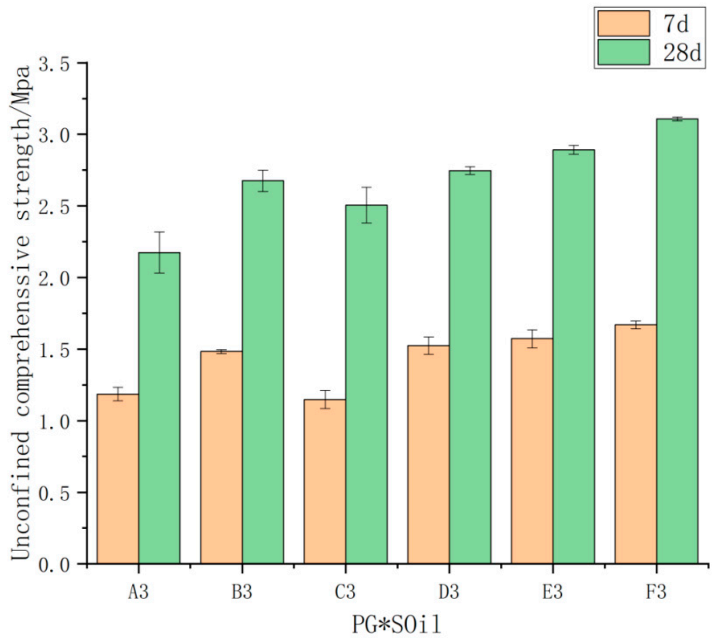

Figure 6. Strength change curves of CaO and GGBS fixed at 4% × 16% with different proportions of phosphogypsum compounded and maintained for 7d and 28d. (* = × means multiplication).

3.4. Stress–Strain Curve

The stress–strain curves of phosphogypsum with different proportions at 7 days and 28 days are depicted in Figure 7b,c, respectively. It can be observed from figure that the stress–strain diagram exhibits four distinct stages, namely elastic rising stage, plastic rising stage, limit stage, and falling stage [27]. Initially, the test sample is compacted and the primary pores in the specimen are compressed, initiating the stable bearing stage. The relationship between stress development and strain approximates a linear pattern with a gradual increase in stress. Simultaneously, the slope of linearity increases with increasing strength value. As strain continues to increase beyond its failure threshold, deformation enters into the second phase of plastic rise where numerous interface cracks appear within the specimen; both their number and length gradually increase as the load intensifies. Brittle failure occurs when solidified soil reaches its ultimate compressive strength. Subsequently, as strain increases further, the curve stabilizes until reaching its peak, at which point it enters into a limit stage characterized by longitudinal cracks parallel to compression direction before transitioning into a descending section, indicating imminent failure of the specimen. Finally, strain continues to increase until complete failure of the test block.

The ultimate stress–strain refers to the state of failure of a material when subjected to external forces, and its value is an important indicator of material toughness and compressive deformation [28]. As depicted in Figure 7b, the stress–strain range for specimens cured for 7 days is 0.8–1.2, while that for specimens cured for 28 days (as shown in Figure 7c) is 0.8–1.5. The stress–strain curves of phosphogypsum with different contents exhibit similar shapes, with no apparent cracks observed prior to reaching the peak load. Upon reaching the peak stress, small cracks become visible and rapidly develop into larger macro cracks. Consequently, there is a rapid decline in load resulting in a steeper stress–strain curve, until the stress drops to approximately 20–30% of the peak stress level. In comparison to those cured for only 7 days, test blocks cured for 28 days display more pronounced brittle failure characteristics primarily due to ongoing internal hydration and other chemical reactions during later stages where internal water consumption persists; however, this leads to denser structure formation and continuous strength enhancement.

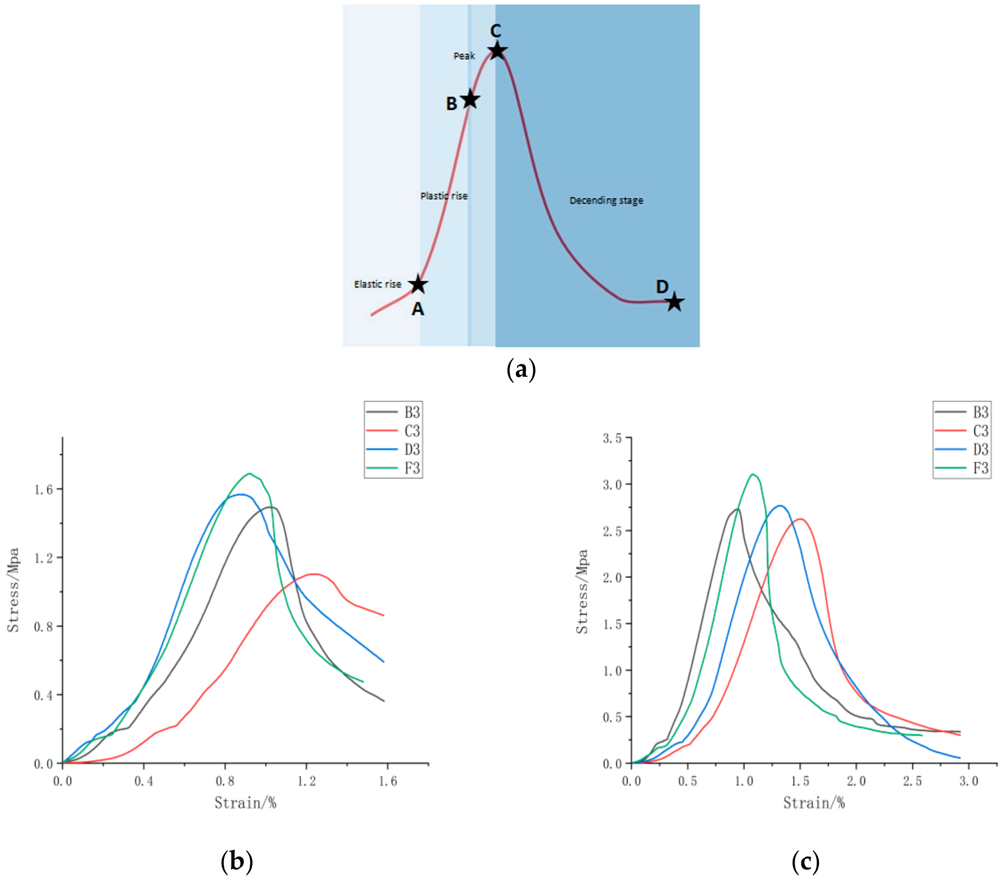

Figure 7. Characteristics of stress–strain curve relationship. (**a**) Schematic diagram of stress–strain curve stages; (**b**) stress–strain curves of CaO and GGBS fixed at 4% × 16% with different proportions of phosphogypsum compounded and maintained for 7d versus 28d; and (**c**) stress–strain curves of CaO and GGBS fixed at 4% × 16% with different proportions of phosphogypsum compounded and maintained for 28d versus 28d.

3.5. Effect of Wet and Dry Cycles on Different Phosphogypsum Dosages

Figures 8 and 9 depict the effects on the cured soil in terms of morphology, mass, and unconfined compressive strength (UCS) after 0, 1, 3, and 5 wet and dry cycles for E2, C3, and F3 curing for 28 d, respectively.

According to the specified conditions of the specimen and as depicted in Figure 9, following one, three, and five cycles of drying and wetting, varying degrees of surface damage were observed. Sample E2 exhibited numerous pores on its surface, which gradually increased in number and size with each cycle, accompanied by the emergence of some cracks. Similarly, sample C3 displayed both pores and cracks on its surface; however, their extent and quantity expanded with an increasing number of cycles, eventually leading to the formation of penetrating cracks. In contrast, sample F3 exhibited the minimal presence of cracks and pores on its surface, which remained largely unaffected by an increase in cycle count, thereby maintaining an overall good condition.

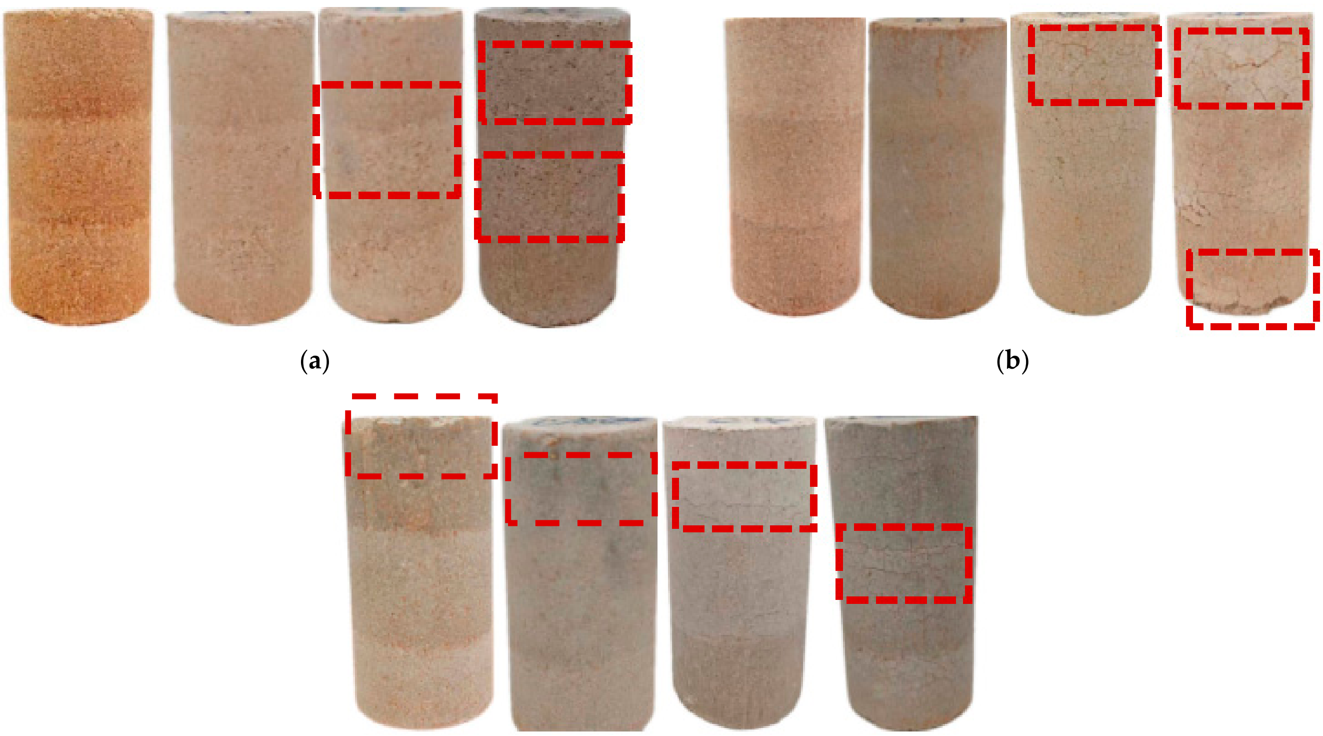

(**a**) (**b**)

(**c**)

Figure 8. Effect of number of wet and dry cycles on the morphology of different phosphogypsum dosages: (**a**) 0% phosphogypsum dosage, (**b**) 20% phosphogypsum dosage, and (**c**) 35% phosphogypsum dosage. The red box shows a schematic box of rupture damage after wet and dry cycling.

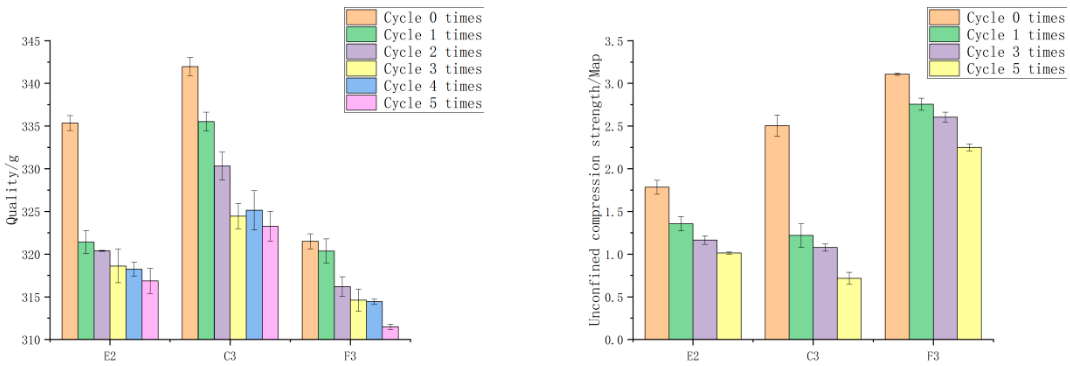

(**a**) (**b**)

Figure 9. (**a**,**b**) The effect of the number of wet and dry cycles on the mass and strength of different phosphogypsum dosages, respectively.

In Figure 9a, the mass change in the three test blocks after undergoing dry–wet cycles is presented. It can be observed that with an increasing number of cycles, the quality of E2 and C3 test blocks experiences a sharp decline after the first cycle, while the quality of F3 test block decreases more gradually. After five dry and wet cycles, the mass reduction percentages for E2, C3, and F3 test blocks were recorded as 5.52%, 5.48%, and 3.11%, respectively. Notably, both E2 and C3 blocks lose an additional 2% in mass compared to F3 blocks.

In Figure 9b, changes in unconfined compressive strength are illustrated. It is evident that there were overall strength decreases for all test blocks following cycling between dryness and wetness conditions. The decline in strength was particularly significant for E2 and C3 test blocks which experienced reductions of 43.18% and 71.39%, respectively. In contrast, the decrease in strength for the F3 test block is relatively smaller at only 27.58%, ranging from 3.107 MPa to 2.2501 MPa.

After undergoing multiple cycles of wetting and drying, the surface of the sample will exhibit varying degrees of deterioration, leading to a decrease in both quality and unconfined compressive strength. However, when compared to E2 and C3, the F3 test blocks demonstrated superior resilience and integrity even after exposure to these environmental conditions.

The aforementioned situation arose due to the repeated soaking and evaporation of water in the sample during the dry–wet cycle, resulting in a disparity in water content between the interior and exterior of the sample. This discrepancy induced tensile stress on the surface of the sample. When there was insufficient cementation among particles within the sample to withstand this tensile stress, voids appeared on its surface. As the cycles progressed, these voids expanded further, leading to the structural degradation of soil and subsequent strength decline. It should be noted that as cycles increased, strength gradually decreased or even exhibited slight improvement. This can be attributed to residual water within the sample after soaking, which promotes hydration reactions during drying processes, thereby increasing hydration products and enhancing internal cementation capacity. Throughout this process, particle bonding became sufficient to resist tensile stresses caused by disparities in the moisture content and strength between both sides of the specimen.

3.6. Microscopic Results Testing

According to Figure 10, the surface of the test block without a phosphogypsum content exhibited numerous pores of varying sizes, calcium hydroxide crystals, and calcium silicate hydrate (C-S-H). This indicates that the combination of calcium oxide and blast furnace slag generates a significant amount of calcium silicate hydrate (C-S-H) and calcium hydroxide. Additionally, it effectively stimulates the activity of blast furnace slag. The test block with 15% phosphogypsum content produces some ettringite. Its internal structure is relatively dense with a smoother surface. There are more pores inside, along with noticeable incomplete penetration of microscopic cracks. A large quantity of ettringite and interwoven calcium silicate hydrate (C-S-H) constantly fill in voids, resulting in a denser internal structure for the specimen.

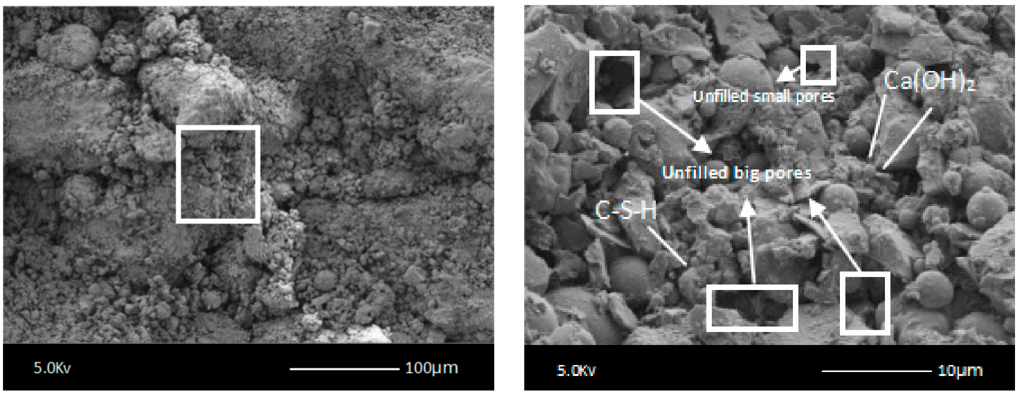

(**a**) 100 μm—0% phosphogypsum dosing (**b**) 10 μm—0% phosphogypsum dosing

Figure 10. *Cont.*

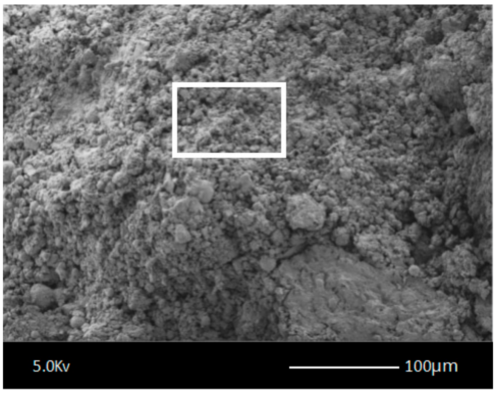

(**c**) 100 µm—15% phosphogypsum dosing

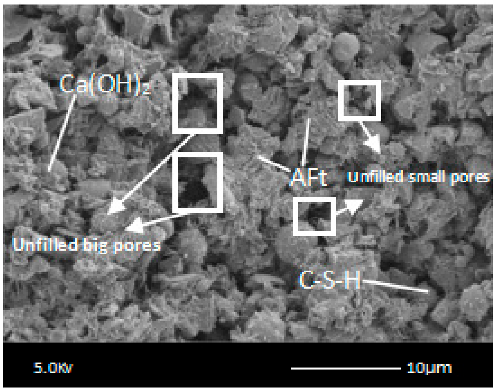

(**d**) 10 µm—15% phosphogypsum dosing

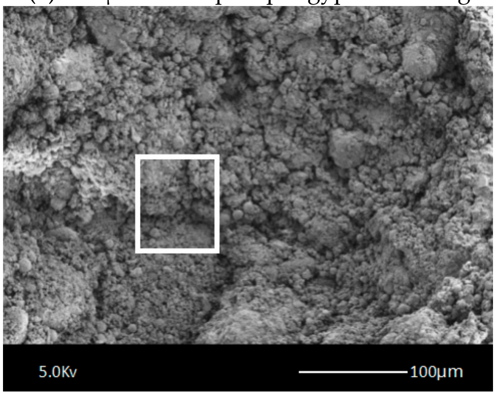

(**e**) 100 µm—20% phosphogypsum dosing

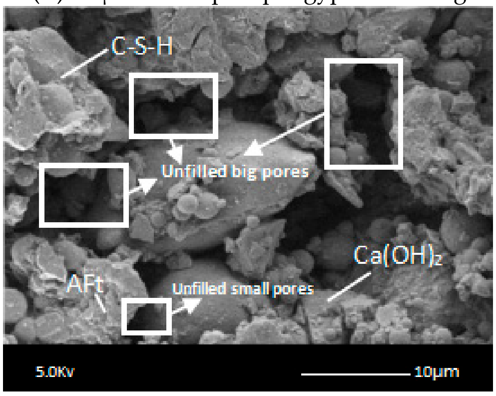

(**f**) 10 µm—20% phosphogypsum dosing

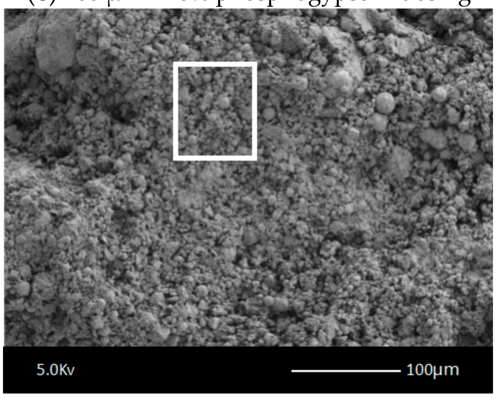

(**g**) 100 µm—25% phosphogypsum dosing

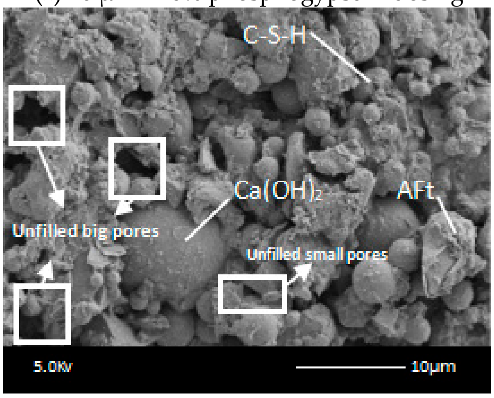

(**h**) 10 µm—25% phosphogypsum dosing

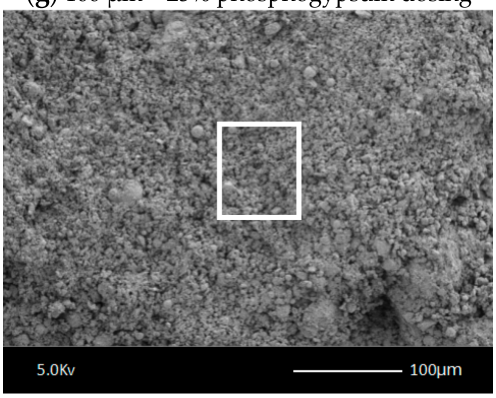

(**i**) 100 µm—35% phosphogypsum dosing

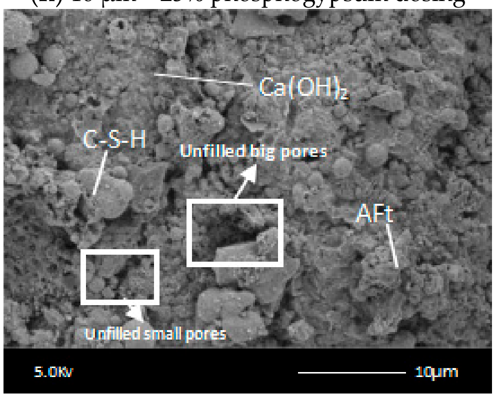

(**j**) 10 µm—35% phosphogypsum dosing

Figure 10. (**a**–**j**) depicts the microstructure of the specimens with different phosphogypsum dosages, respectively.

Simultaneously, this greatly enhances the gelling material properties of blast furnace slag and improves the strength of the test block. In case of a test block containing 20% phosphogypsum content, gypsum crystals form on both its surface and interior. Furthermore, there are various-sized pores present due to excessive gypsum which fails to react with other materials in the system. These unreacted gypsum particles distribute in a disorderly manner within the internal system, forming larger and smaller pores that ultimately reduce strength. For a test block consisting of a 25% phosphogypsum content, fewer large pores are observed while small pore quantities remain relatively unchanged compared to previous cases. The presence or quantity variation in ettringite is minimal. In contrast, when using a 35% phosphogypsum content as part "soil", it not only acts as a curing agent but also fills up pore spaces as its concentration increases, gradually sanding down structures.

In the test block containing 0–15% phosphogypsum, a certain amount of ettringite was detected without any discernible alteration in the interior. However, the formation of ettringite crystals increased the quantity of calcium silicate hydrate (C-S-H) while decreasing that of calcium hydroxide. The combination of ettringite crystals and C-S-H improved specimen strength. At 15–20%, new gypsum appeared, with a significant increase in calcium hydroxide production; excessive phosphogypsum resulted in larger pores and lower strength. Although pores still existed at 20–25% content, they gradually decreased over time. At 20–35%, few internal pores remained as excess phosphogypsum filled them up; there was also an increase in both calcium hydroxide and C-S-H.

3.7. Economy, Benefit and Radioactive Safety Analysis

In the analysis of unconfined compressive strength, the preliminary experiment showed that the plain soil reacted with 5% cement achieved a strength of 1.85 MPa at 7 days and 3.15 MPa at 28 days. Currently, the mixture of 4% calcium oxide *16 blast furnace slag *35% phosphogypsum exhibited a strength of 1.670 MPa at 28 days and 3.107 MPa at 7 days in curing, with similar strengths observed between both time periods. Furthermore, this material meets the requirements for the unrestricted compressive strength of certain stable inorganic binders and can be applied in practical engineering.

In the economic analysis, based on the current market price, the unit price of concrete is CNY 350 yuan per ton, while calcium oxide is priced at approximately CNY 270 per ton. Blast furnace slag and phosphogypsum are classified as industrial waste, with blast furnace slag costing between CNY 7 and 15 per ton. Currently, for every 1 ton of phosphoric acid produced by chemical industry manufacturers in China, around 4.5–5 tons of phosphogypsum are generated; therefore, the actual trading value of phosphogypsum is negligible. Considering the materials required for the specific project, both blast furnace slag and phosphogypsum costs can be disregarded along with potential alternatives to sand and stone usage. The construction cost for one meter of secondary highway amounts to CNY 1500 and requires nearly 2.8 tons of concrete per meter. Based on the aforementioned experimental scheme, savings of approximately CNY 744 can be achieved per meter.

However, Essaid Bilal [29] believes that m-PG (especially m-PG from Russia and some PG from China) usually shows a relatively low radioactivity index of 0.24–0.45. So the radioactive safety problem is also in line with the actual construction situation.

At the same time, for solid wastes such as engineering muck, blast furnace slag and phosphogypsum, we can also consider using fly ash and rice husk ash replace [30], which can also be mixed with wood fiber [31] and other wastes to strengthen the curing effect.

Considering durability, mechanical properties, and cost-effectiveness, calcium oxide, blast furnace slag and phosphogypsum can be selected as 4%X16%X (25% PGX75% Soil) or 4%X16%X (35% PGX65% Soil), in accordance with the "Technical Standards for Soil Curing Agent Application". The standard requires a minimum base strength of $\geq$2.5 MPa on the road. According to the results of this study, the above two test blocks can meet the requirements; combined with the economic comparison results, the optimal calcium oxide * blast furnace slag * phosphogypsum is 4%X16%X (25% PGX75% Soil). The Technical Standard for Application of Soil Curing Agent requires that the strength of road subbase is

≥1.5 MPa. According to the results of this study, combined with the results of economic comparison, both samples meet the requirements.

4. Conclusions

In this study, three additives, namely calcium oxide, waste phosphogypsum, and blast furnace slag, were incorporated into the soil samples from the Weishui Town Highway reconstruction project to enhance the stabilization of loess in the experimental setup. The specific findings are presented as follows:

(1) The results of the unconfined compressive strength tests demonstrate that the incorporation of phosphogypsum and blast furnace slag facilitates the formation of C-S-H gel, which reacts with calcium oxide to generate needle-like ettringite. The reaction between calcium oxide, blast furnace slag, and phosphogypsum produces C-S-H gel and calcium silicate hydrate. Furthermore, the addition of 35% phosphogypsum significantly enhances the compressive strength of cement. Additionally, as the curing age increases, there is a notable improvement in the stability of loess. Specifically, when comparing temperatures at 7 days and 28 days, there is an increase in compressive strength from 1.670 MPa to 3.107 MPa.

(2) The unconfined compressive strength and durability of the sample can be significantly enhanced by adjusting the phosphogypsum content, following dry and wet cycling. Observations after the cycles revealed distinct phenomena for samples with no phosphogypsum, and a low and high content: samples without any phosphogypsum exhibited a notable increase in porosity along with a moderate decline in quality and strength; samples with a low content displayed rapid expansion of appearance fissures, indicating signs of fracture accompanied by substantial loss in quality and strength; high-content samples showed minimal changes in crack formation after the third cycle but experienced significant increases after the fifth cycle, still demonstrating improvement compared to those with no or low content while experiencing minimal loss in quality and strength.

(3) The construction conditions allow for the selection of two ratios of calcium oxide, blast furnace slag, and phosphogypsum: 4% CaO × 16% BFS × (25% PG × 75 Soil) and 4% CaO × 16% BFS × (35% PG × 65 Soil). This choice can result in an economic saving of CNY 744 per meter.

(4) The SEM observation reveals that the reaction between calcium oxide and blast furnace slag generates ettringite and C-S-H gel, which can effectively interact with $Ca(OH)_2$ in quicklime to establish the initial structure and provide early strength for the sample. In an alkaline environment, phosphogypsum is activated to produce a certain amount of C-S-H gel and ettringite, thereby filling material gaps and accelerating the formation of hydration products at appropriate stages, ultimately resulting in a compact microstructure.

However, there are still many materials in the research field that have not been heavily invested, such as clay containing kaolinite and the inorganic polymer of silicon aluminum chain. We still need to continue to explore new materials, and can continue to innovate and progress in terms of practicality, economy and durability.

Author Contributions: Conceptualization, Y.F. and F.W.; methodology, Y.F., F.W. and W.Y.; validation, Y.F., F.W. and W.Y.; formal analysis, F.W.; investigation, F.W.; resources, Y.F.; data curation, F.W. and Y.F.; writing—original draft preparation, J.W.; writing—review and editing, Y.F. and J.W.; visualization, J.W. and Y.F.; supervision, Y.F. and F.W.; project administration, J.W. and Y.F.; funding acquisition, Y.F. All authors have read and agreed to the published version of the manuscript.

Funding: The authors are thankful for the financial support from the National Natural Science Foundation of China (No. 52108315) and the National Science Foundation of Hubei Province of China (2021CFB286).

Data Availability Statement: The data presented in this study are available in the article.

Acknowledgments: We wish to thank the anonymous referees for their careful reading and for providing insightful comments to improve the initial version of this paper.

Conflicts of Interest: The authors declare no conflict of interest.

References

1. Xing, Z. Analysis of engineering geological characteristics of soft soil embankment foundation of Xiashan Lake embankment in Wuhan. *Northwest Hydropower* **2019**, *1*, 26–29+34.
2. Zhang, B. Analysis of the causes of instability of embankment foundation in a project with soft land base. *Zhihuai* **2014**, *7*, 16–18.
3. Huang, X.; Zhou, G. A preliminary study on the hardening mechanism of cement-reinforced soil. *J. Geotech. Eng.* **1994**, *1*, 62–68.
4. Liang, S.; Luo, Q.; Wang, M. Experimental study on lime and cement curing of zinc-polluted soft soil in Nansha. *J. Guangdong Univ. Technol.* **2017**, *34*, 80–85.
5. Saadeldin, R.; Siddiqua, S. Geotechnical characterization of a clay-cement mix. *Bull. Eng. Geol. Environ.* **2013**, *72*, 601–608. [CrossRef]
6. Miao, X.; Lu, Y.; Fu, R.; Kong, D.; Fu, R.; Hu, Q. Preparation of composite cementitious materials by semi-aqueous phosphogypsum involved in curing as-received phosphogypsum. *Inorg. Salt Ind.* **2022**, *54*, 10–16. [CrossRef]
7. Dong, J.; Jiang, M.; Zhao, X. Performance and mechanism of modified β-phosphogypsum hemihydrate in curing lead-containing sludge. *Chem. Environ. Prot.* **2022**, *42*, 231–236.
8. Bian, X.; Zeng, L.; Ji, F.; Xie, M.; Hong, Z. Plasticity role in strength behaviour of cement-phosphogypsum stabilized soils. *J. Rock Mech. Geotech. Eng.* **2022**, *14*, 1977–1988. [CrossRef]
9. Zhang, B. *Research on Key Technology of Roadbed Construction of Engineering Waste Soft Soil Curing Material*; CCCC Water Conservancy and Hydropower Construction, Co.: Beijing, China, 2021.
10. Yi, Y.; Liska, M.; Jin, F.; Al-Tabbaa, A. Mechanism of reactive magnesia—Ground granulated blastfurnace slag (GGBS) soil stabilisation. *Can. Geotech. J.* **2015**, *53*, 773–782. [CrossRef]
11. Sun, B. *Research on Optimisation of Curing Formulations for Soft Soil in Hefei Lake Deposit*; Anhui University of Architecture: Hefei, China, 2017.
12. Wang, Z. *Optimisation Study of Soft Soil Formulation Based on GGBS Curing Wuhu*; Anhui University of Architecture: Hefei, China, 2019.
13. Ma, S. *Optimisation of Curing Formulations and Mechanical Properties of Wuhu Silty Clay*; Anhui Architecture: Huangshan, China, 2022. [CrossRef]
14. Dong, W.; Zhan, Q.; Zhao, X.; Wang, A.; Zhang, Y. Study on the solidification property and mechanism of soft soil based on the industrial waste residue. *Rev. Adv. Mater. Sci.* **2023**, *62*, 20220303. [CrossRef]
15. *JTG E40-2007*; Test Methods of Soils for Highway Engineering. Code. Chinese Standard GB/T: Beijing, China, 2007.
16. *JTG40-2011*; Design Specification for Highway Cement Concrete Pavement. Chinese Standard GB/T: Beijing, China, 2011.
17. Zimmermann, I.; Filser, S.; Mordhorst, A.; Fleige, H.; Horn, R. Structural stabilisation of soil backfill with quicklime. *J. Plant Nutr. Soil Sci.* **2019**, *182*, 578–585. [CrossRef]
18. Siaw, F.A.; Wang, H.; Feng, H.; Cheng, L.; Feng, L.Z. Use of Taguchi method to evaluate the unconfined compressive strength of quicklime stabilised silty clayey subgrade. *Case Stud. Constr. Mater.* **2022**, *17*, e01417.
19. Sharma, K.A.; Sivapullaiah, P. Ground granulated blast furnace slag amended fly ash as an expansive soil stabiliser. *Soils Found.* **2016**, *56*, 205–212. [CrossRef]
20. Zhang, Z.; Lian, F.; Ma, L.; Jiang, Y. Effects of Quicklime and Iron Tailings as Modifier on Composition and Properties of Steel Slag. *J. Iron Steel Res. Int.* **2015**, *22*, 15–20. [CrossRef]
21. Obuzor, G.; Kinuthia, J.; Robinson, R. Enhancing the durability of flooded low-capacity soils by utilising lime-activated ground granulated blastfurnace slag (GGBS). *Eng. Geol.* **2011**, *123*, 179–186. [CrossRef]
22. Wareham, D.G.; Mackechnie, J.R. Solidification of new zealand harbor sediments using cementitious materials. *J. Mater. Civ. Eng. J. Mater. Civ. Eng.* **2006**, *18*, 311–385. [CrossRef]
23. Chrysochoou, M.; Grubb, D.G.; Drengler, K.L. Stabilised dredged material. III: Mineralogical perspective. *J. Geotech. Geoenviron. Eng.* **2010**, *136*, 1037–1050. [CrossRef]
24. Ding, J.; Zhang, S.; Hong, Z. Experimental study of solidification of dredged clays with high water content by adding cement and phosphogypsum synchronously. phosphogypsum synchronously. *Rock Soil Mech.* **2010**, *31*, 2817–2822.
25. Djayaprabha, H.S.; Nguyen, H.A. Utilising phosphogypsum waste to improve the mechanical and durability performances of cement-free structural mortar containing ground granulated blast furnace slag and calcium oxide. *J. Build. Eng.* **2023**, *72*, 106557.
26. Park, H.; Jeong, Y.; Jun, Y.; Jeong, J.-H.; Oh, J.-E. Strength enhancement and pore-size refinement in clinker-free CaO-activated GGBFS systems through substitution with gypsum. *Cem. Concr. Compos.* **2016**, *68*, 57–65. [CrossRef]
27. Wang, W.; Zhao, Q.; Zhang, D.; Chen, P. Effect of relative humidity on the tensile properties of GFRP bars inseawater sea sand concrete environment. *J. Shanghai Jiao Tong Univ.* **2023**, *57*, 148–160. [CrossRef]
28. Li, L.-H.; Han, Q.-P.; Yang, X.; Xiao, H.L.; Li, W.T.; Huang, S.P. Research on mechanical properties and micro-mechanism of rice husk ash-cement cured silt soil. *J. Civil Eng.* **2023**, *56*, 166–176. [CrossRef]

29. Bilal, E.; Bellefqih, H.; Bourgier, V.; Mazouz, H.; Dumitraş, D.-G.; Bard, F.; Laborde, M.; Caspar, J.P.; Guilhot, B.; Iatan, E.-L.; et al. Phosphogypsum circular economy considerations: A critical review from more than 65 storage sites worldwide. *J. Clean. Prod.* **2023**, *414*, 137561. [CrossRef]
30. Mahdi, S.M.; Babu, D.V.; Hossiney, N.; Abdullah, M.M.A.B. Strength and durability properties of geopolymer paver blocks made with fly ash and brick kiln rice husk ash. *Case Stud. Constr. Mater.* **2022**, *16*, e00800. [CrossRef]
31. Puangrat, S.K.K. Comparative microstructures and mechanical properties of mortar incorporating wood fiber waste from various curing conditions. *Case Stud. Constr. Mater.* **2022**, *16*, e00855.